Popping Balloons: A Case Study of Dynamical Fragmentation

Sébastien Moulinet and Mokhtar Adda-Bedia
*Laboratoire de Physique Statistique, Ecole Normale Supérieure, UPMC Paris 6, Université Paris Diderot,
CNRS, 24 rue Lhomond, 75005 Paris, France*

Understanding the physics of fragmentation is important in a wide range of industrial and geophysical applications. Fragmentation processes involve large strain rates and short time scales that take place during crack nucleation and propagation. Using rubber membranes, we develop an experimental analysis that enables us to track the fragmentation process *in situ* in both time and space. We find that bursting a highly stretched membrane yields a treelike fragmentation network that originates at a single seed crack, followed by successive crack tip-splitting events. We show that a dynamic instability drives this branching mechanism. Fragmentation occurs when the crack tip speed attains a critical velocity for which tip splitting becomes the sole available mechanism of releasing the stored elastic energy. Given the general character of the fragmentation processes, this framework should be applicable to other crack networks in brittle materials.

Fragmentation encompasses a wide spectrum of physical processes that occur in both human activities and natural phenomena. Besides liquid atomization [1], examples where matter is fragmented into smaller pieces abound, such as breakup of heavy nuclei [2], comminution [3], armor penetration, shell case bursting [4], meteoric cratering [5,6], and collision of asteroids [7]. The academic interest originates from the association of fragmentation processes with understanding both the dynamics of crack propagation [8–10] and the various ways of partitioning a given topology into smaller discrete entities [11]. Since Mott's seminal observations and theoretical concepts [4,11], fragmentation of ductile and brittle solids under high strain rates has been a topic of intense research [11–16]. The main objective of these studies is the theoretical prediction of the distribution of fragment sizes resulting from a fragmentation event. However, the extreme conditions associated with large strain rates and small time scales involved in crack nucleation events and dynamics make experimental studies challenging and thus prevent the emergence of a clear scenario of the fragmentation process.

Our study stems from a phenomenon that everyone can observe (see Fig. 1 and Movie 1 in Ref. [17]). When a moderately inflated toy balloon is pricked, a crack races around it, slicing the membrane into few fragments. The crack either runs straight or curved or wiggles, leaving different patterns on the edges of the fragments [19,20]. On the other hand, a highly tensed balloon bursts into a large number of shreds, whether the explosion is spontaneous or triggered. A natural question that arises is, what drives the transition from a single crack propagation to a fragmentation process? While illustrations of balloon fragmentation are ubiquitous, we are not familiar with a controlled study of this phenomenon.

In order to have a more tractable system than a commercial rubber balloon, we have devised an experiment to perform the fragmentation of latex membranes. A flat sheet of natural rubber, whose thickness ranges from 350 to 1100 μm, is clamped to a circular frame of diameter 52 mm (Fig. 1). The front side of the frame is opened to allow the expansion of the membrane and the closed rear side is connected to a compressed air inlet. When air is injected, the sheet stretches, taking the form of a growing axisymmetric balloon, characterized by an equatorial radius r_{max}, until it hits an acute indenter (X-ACTO blade) that triggers the explosion. In all experiments, the tip of the blade is placed on the axis of symmetry of the inflated membrane, so that the cracks propagate away from the "pole" of the balloon. The control parameter of the experiment is the distance between the indentor and the frame and prescribes the stored elastic energy in the membrane. If the blade is positioned far enough away, the balloon may pop spontaneously and fragmentation nucleates at a random position. In the study of rubber fracture, crystallization is known to yield irreversible deformations [21], and working at high temperatures allows us to avoid this effect [22]. Instead, we have chosen to rapidly inflate the membrane such that the experiment lasts less than 15 s. We have checked the effectiveness of this protocol by examining that the fragments of the *postmortem* samples recover their initial size with a residual elongation smaller than 5%. Using a fast camera (Photron APX RS) that is placed in front of the setup (camera 1 in Fig. 1), the explosion of the membrane is recorded at frequencies of 30 000 fps or 60 000 fps. A second camera (camera 2 in Fig. 1) working at 25 fps records a side view of the balloon while a sensor connected to the frame monitors the overpressure ΔP. Combining the side view imaging and the pressure measurement allows a
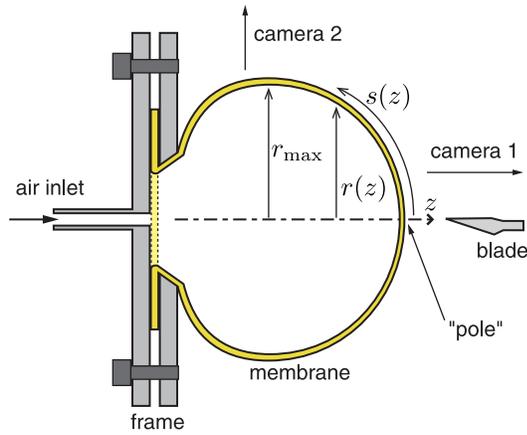
FIG. 1 (color online). Cross section of the experimental setup. The dotted line represents the initial flat state of the latex sheet before its inflation. Notations for the inflated membrane: $s(z)$ represents the arc length and $r(z)$ the distance to the axis of symmetry.

measurement of the tension T in the membrane (see methods in Ref. [17]).

Similarly to toy balloons, two different behaviors are observed in our experiment (Movie 2 in Ref. [17]). The first case corresponds to an opening regime that occurs for a short distance between the blade and the frame [Fig. 2(a)]. Once the membrane meets the blade, a hole is formed and expands with the progression of two or three radial cracks cutting the sample into a few large fragments. The second case corresponds to the fragmentation regime and occurs when the explosion is either spontaneous or triggered by a blade placed beyond a critical distance. Several cracks expand radially from the initial puncture [Fig. 2(b)], turning the membrane into a large number of fragments in the shape of elongated shreds (our current best is 64 fragments).

The analysis of the postmortem samples reveals the scenario leading to a large number of fragments. Figure 2(c) shows that the crack network form a treelike structure with junctions of Y shape and that only a few fragments emanate from the center of the sample. This observation proves that the whole crack network is not nucleated at the initial puncture but results from several branching events during a fragmentation process. The fast imaging confirms this scenario: in the first image on Fig. 2(b), only four cracks are present while 14 can be counted 67 μs later. Figure 2(d) shows the mechanism of generation of new cracks: an initial single crack splits spontaneously, giving birth to two branches that can in turn split again. Therefore, the large number of fragments originates from a germ of two or three crack tips that undergoes successive tip-splitting events. For all experiments, the tip-splitting events occur in the region of the balloon limited by $r \lesssim 0.8 r_{\max}$ and additional branching is rarely observed beyond it.

The phenomenon of branching is a generic dynamic instability of crack propagation in a variety of different
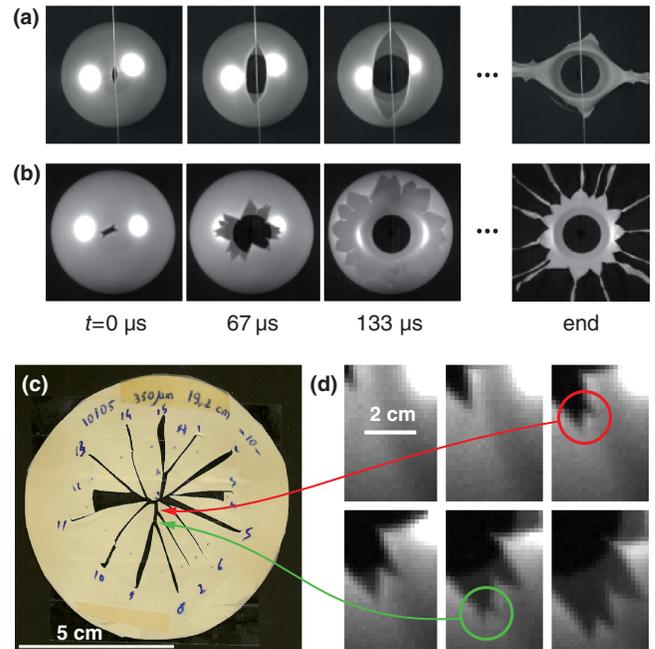

FIG. 2 (color online). The two different regimes of explosion are visualized using fast imaging. (a) Opening regime. A single fracture splits the membrane in two. The vertical line appearing on the images is the rod that supports the blade used to trigger the explosion. (b) Fragmentation regime. From a single initial fracture, a network of cracks develops, eventually turning the membrane into numerous shreds (presently 15). In this example, the explosion is spontaneous. In (a) and (b), the dark disk in the center of the images is the circular frame, its inner diameter (52 mm) sets the scale. (c) Postmortem sample ($e = 350$ μm). (d) Close-up extracted from the movie corresponding to the sample shown in (c). The time interval between two successive images is $1/60\,000$ s. Two successive tip splittings has turned an initial single crack into three cracks. The colored circles and arrows indicate the corresponding events on the postmortem sample.

brittle materials [9,10,23]. Beyond a critical velocity a single crack can undergo local crack branching events, where a single mother crack gives birth to successive short-lived daughter cracks. Some aspects of this instability, known as the microbranching instability, are described in the framework of linear elastic fracture mechanics [24,25]. Using energy balance arguments, the branching of a single crack propagating in a two-dimensional material is found to be energetically possible when its speed exceeds a certain critical value. However, this approach focuses on a scenario of a two-dimensional crack tip splitting, while micro-branching appears to be intrinsically a three-dimensional instability [9,10]. In the footsteps of the classical branch-ing, the following will address the fragmentation problem in terms of loading and dynamics.

The final number N_f of cracks depends on both the applied tension T and the initial membrane thickness e [17]. Nevertheless, membranes with different thicknesses exhibit
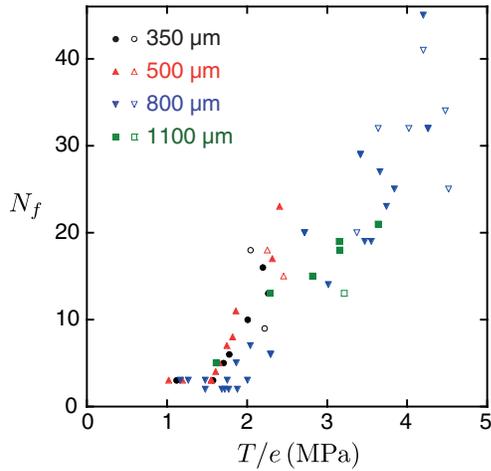
FIG. 3 (color online). Final number of cracks N_f as a function of the ratio T/e, where T is the membrane tension measured at the pole of the balloon and e the initial membrane thickness. The results for four different thicknesses are displayed. Filled (open) symbols represent triggered (spontaneous) explosions. Since each measurement of T/e has a relative uncertainty of the order of 2%, the dispersion of the data points illustrates the stochastic aspect of the fragmentation.

the same behavior. For small tensions, a plateau at 2 or 3 final cracks is observed and corresponds to the opening regime. Above a critical tension T_c, the final number of cracks increases quasilinearly with T. Figure 3 shows that the number of cracks varies with the single parameter T/e and that the transition from opening to fragmentation regimes is controlled by a critical value $T_c/e = 1.8 \pm 0.2$ MPa. Thus, the physical control parameter of the fragmentation process is the stress experienced by the membrane. One notes that T/e is not the actual stress, as a stretched membrane gets thinner. Assuming that rubber is an incompressible material, the actual stress in the material is given by $\sigma = T\lambda^2/e$, where λ is the strain, defined as the ratio of the stretched length to the original length. In the fragmentation regime, the value of λ is estimated by comparing the distance that separates two consecutive tip-splitting events on the fast camera movies and the length of the corresponding crack on the postmortem samples. Within the accuracy of this method, we find that in all samples $\lambda = 7.0 \pm 0.5$ independently of the applied tension. This value appears to be a limiting strain. Indeed, a divergence of the tension at a finite stretch is expected when the polymeric chains of the material reach their maximal extension [26]. One concludes that the fragmentation process occurs when the material experiences a tensile stress larger than a threshold $\sigma_c = 88 \pm 15$ MPa.

In addition to material loading, dynamics is a key feature to understand fast propagating cracks and their potential branching [10]. The fast imaging allows us to follow the instantaneous crack extension during the explosions. In the opening regime and over the region of interest, we find that

cracks progress at a constant speed that increases with the membrane tension T [Fig. 4(a)]. Similar crack dynamics behavior has been observed in flat membranes submitted to anisotropic stretching of magnitude smaller than that reached in our experiments [22,27]. In the fragmentation regime, the tip splitting hinders the following of a single crack. Nevertheless, due to the triggering at the pole of the inflated membrane, the instantaneous radial lengths of all cracks are equal within the experimental accuracy. Figure 4(a) shows that the extensions $s(t)$ of the crack network for various tensions $T > T_c$ are superimposed straight lines, confirming that the velocity in the fragmentation regime is not only constant over the network development but is also independent of the membrane tension. These experimental results show that when the stress in the membrane attains the threshold σ_c, the crack propagation reaches a limit velocity $v_l = 570 \pm 15$ m/s. At larger stresses, a single crack does not increase its speed; instead, it undergoes a tip-splitting instability. This behavior raises the question of the nature of the transition whether it is controlled by a dynamic or a mechanical instability.

A striking feature of the cracks that is illustrated in Figs. 2(a) and 2(b) is their V-shaped opening, confirming that cracks propagate at velocities larger than the shear wave speed c_S of the material [22]. The cracks are thus intersonic since their velocities are upper bounded by the longitudinal wave speed c_L of the material. One concludes that in the opening regime a single crack is propagating at a constant intersonic velocity that increases with the applied tension [27]. At the transition to the fragmentation regime, a limiting velocity is observed above which a single crack becomes unstable. It is natural to associate this limiting velocity to the upper limit of the intersonic domain, i.e., the longitudinal wave speed c_L. The assumption $v_l = c_L$ is also consistent with the examination that the membrane ahead of the tips of the cracks remains undeformed until the arrival of the fracture network. Even if they need to be confirmed by direct measurements of the wave speeds, these results confirm that the transition to the fragmentation regime is driven by a dynamic instability.

Admitting that fragmentation occurs with all cracks propagating at the terminal velocity c_L allows us to perform a quantitative characterization of the latex fracture energy Γ under extreme loading. The stored elastic energy in the area $A(t)$ of the spherical cap that encompasses the crack network at time t is estimated by $E_{el} = TA(t)$. Since the cracks propagate at the longitudinal wave speed c_L, only the part of the membrane inside the area $A(t)$ releases stresses while the rest of the balloon remains at its inflated state. Thus, the variation of the elastic energy during an extension ds of the crack network is given by

$$dE_{el} = TdA(t) = 2\pi Tr(t)ds. \qquad (1)$$

This energy should be compared to the work done for the creation of a new fracture area. Crack progression by a
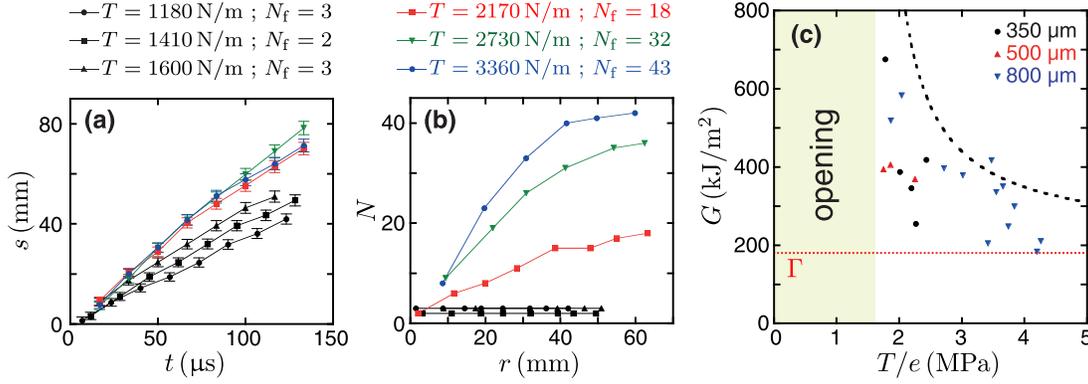
FIG. 4 (color online). (a) Distance $s(t)$ covered by the fractures since their creation for membranes with initial thickness $e = 800\ \mu$m. Black symbols represent the progression of cracks in the opening regime. The velocity is constant and increases with the tension of the membrane. Colored symbols represent the progression of the extremity of a crack network in the fragmentation regime. The cracks propagate at a constant velocity, now independent of the membrane tension. The limit velocity is $v_l = 570 \pm 15$ m/s. (b) Number N of cracks as a function of the coordinate r for experiments with $e = 800\ \mu$m. In the opening regime (black symbols), the number of cracks is constant. In the fragmentation regime (colored symbols), N starts to increase linearly and eventually saturates. Panels (a) and (b) display data from the same experiments and share the same symbols. (c) Values of G as defined by Eq. (3) as a function of T/e. As the calculation holds for the fragmentation regime, no data point is displayed in the opening regime (colored rectangle). The dashed line represents the behavior of G that is consistent with the data of Fig. 3. The red dotted line indicates the estimate of Γ as the asymptotic value of G.

distance ds on the stretched balloon corresponds to an area eds/λ in the unstretched membrane. The energy dissipated for the creation of this new fracture surface is then given by

$$dE_d = N(t)\Gamma e \frac{ds}{\lambda}, \qquad (2)$$

where $N(t)$ is the instantaneous number of cracks in the network. The elastic energy released during crack extension should be larger than the dissipated energy for crack opening: $dE_{\mathrm{el}} \geq dE_d$. Indeed, the excess energy that is not included in the energy balance is the one released during relaxations of the ragged membrane inside the area $A(t)$. This inequality gives an upper limit for the value of Γ:

$$\Gamma \leq G \equiv \frac{2\pi\lambda T}{e}\frac{r(t)}{N(t)}. \qquad (3)$$

To be physically relevant, the elastic energy release rate G, thus the ratio $r(t)/N(t)$, should be time independent. Figure 4(b) shows that, during the early stages of the explosion, the number of cracks $N(t)$ increases linearly with distance $r(t)$ and reaches a maximum value N_f at $r_f \approx 50$ mm, beyond which tip-splitting events are rare. The energy release rate can then be estimated using the slopes of $N(r)$ at small times. Data points in Fig. 4(c) represent these values for several experiments with membranes of different thicknesses. The dashed curve in Fig. 4(c) corresponds to the approximation $r(t)/N(t) \approx r_f/N_f$ with N_f extracted from a linear fit of the data shown in Fig. 3(e). Both methods display a decrease of G with T/e, thus with the number of cracks.

To rationalize the behavior of G, one notices that due to the radial geometry of fracture, a small number of cracks in the network leaves in its wake large triangular sections of the membrane under tension [see Fig. 2(b)]. The corresponding stored elastic energy is released through kinetic relaxation (vibrations, coiling, etc.). When the number of cracks increases, the total area of these sections decreases and the energy that is actually dissipated for fracture becomes closer to G. Therefore, an estimate for the fracture energy Γ is given by the asymptotic value of G for a large number of cracks, or equivalently for large T/e. Using the experimental results of Fig. 4(c), we find $\Gamma \approx 190$ kJ/m^2, which is very large compared to the energy needed to break chemical bonds (≈ 1 J/m^2) and to the fracture energy of torn rubber sheets. Indeed, using the "trouser" test [28], we measured a fracture energy that ranges from 18 to 50 kJ/m^2. Nevertheless, a dependance of Γ with crack tip speed in rubber has been observed in peeling and tearing experiments and was interpreted in terms of viscoelastic dissipation [29]. At fixed temperature, Γ increases with the crack velocity v in proportion to $v^{0.24}$ [30]. Extrapolating the results of the tearing experiment, for which the crack progresses through a succession of jumps of typical speeds $v \approx 1$ m/s, yields a fracture energy at $v = c_L$ that is consistent with our measurements.

Similarly to rubber membranes, the formation of a treelike crack network is a generic feature in impacted brittle materials [8,9]. Although fragmentation occurs at subsonic crack speeds, the process of dynamical instability we have described is a common behavior between these different systems. Consequently, the prediction of the distribution of fragment sizes resulting from a fragmentation process does

not only involve given rules of geometric division of a surface [11] but it should also include modeling of dynamical processes leading to branching instabilities.

---

[1] E. Villermaux, Annu. Rev. Fluid Mech. **39**, 419 (2007).

[2] C. B. Das, S. Das Gupta, W. G. Lynch, A. Z. Mekjian, and M. B. Tsang, Phys. Rep. **406**, 1 (2005).

[3] P. Rosin and E. Rammler, J. Inst. Fuel **7**, 29 (1933).

[4] N. F. Mott, Proc. R. Soc. A **189**, 300 (1947).

[5] H. J. Melosh, *Impact Cratering: A Geologic Process* (Oxford University Press, New York, 1989).

[6] A. Sagy, J. Fineberg, and Z. Reches, J. Geophys. Res. **109**, B10209 (2004).

[7] E. V. Ryan, Annu. Rev. Earth Planet Sci. **28**, 367 (2000).

[8] R. B. Lawn, *Fracture of Brittle Solids* (Cambridge University Press, Cambridge, England, 1993).

[9] K. Ravi-Chandar, *Dynamic Fracture* (Elsevier Science, New York, 2004).

[10] E. Bouchbinder, J. Fineberg, and M. Marder, Annu. Rev. Condens. Matter Phys. **1**, 371 (2010).

[11] D. E. Grady, *Fragmentation of Rings and Shells* (Springer-Verlag, Berlin, 2006).

[12] F. Wittel, F. Kun, H. J. Herrmann, and B. H. Kröplin, Phys. Rev. Lett. **93**, 035504 (2004).

[13] F. P. M. dos Santos, V. C. Barbosa, R. Donangelo, and S. R. Souza, Phys. Rev. E **81**, 046108 (2010).

[14] H. Zhang and K. Ravi-Chandar, Int. J. Fract. **142**, 183 (2007).

[15] H. Zhang and K. Ravi-Chandar, Int. J. Fract. **150**, 3 (2008).

[16] N. Vandenberghe, R. Vermorel, and E. Villermaux, Phys. Rev. Lett. **110**, 174302 (2013).

[17] See Supplemental Material at http://link.aps.org/supplemental/10.1103/PhysRevLett.115.184301, which contains Ref. [18], for movies, method for measuring the membrane tension and additional figures.

[18] I. Müller and P. Strehlow, *Rubber and Rubber Balloons* (Springer, Berlin, 2004).

[19] A. Stevenson and A. G. Thomas, J. Phys. D **12**, 2101 (1979).

[20] R. D. Deegan, P. J Petersan, M. Marder, and H. L. Swinney, Phys. Rev. Lett. **88**, 014304 (2001).

[21] P. J. Flory, J. Chem. Phys. **15**, 397 (1947).

[22] C. H. Chen, H. P. Zhang, J. Niemczura, K. Ravi-Chandar, and M. Marder, Europhys. Lett. **96**, 36009 (2011).

[23] H. Henry and H. Levine, Phys. Rev. Lett. **93**, 105504 (2004).

[24] M. Adda-Bedia, J. Mech. Phys. Solids **52**, 1407 (2004).

[25] E. Katzav, M. Adda-Bedia, and R. Arias, Int. J. Fract. **143**, 245 (2007).

[26] A. N. Gent, Rubber Chem. Technol. **69**, 59 (1996).

[27] P. J. Petersan, R. D. Deegan, M. Marder, and H. L. Swinney, Phys. Rev. Lett. **93**, 015504 (2004).

[28] R. S. Rivlin and A. G. Thomas, J. Polym. Sci. **10**, 291 (1953).

[29] A. N. Gent, Langmuir **12**, 4492 (1996).

[30] A. N. Gent, *The Science and Technology of Rubber* (Elsevier, New York, 2005).